Maternal hormones engage a dormant monomorphic aggression circuit, leading to the introduction of an innate behavior in adulthood in females

Stefanos Stagkourakis[1,,¶], Paul Williams[2], Giada Spigolon[1], Shreya Khanal[1], Katharina Ziegler[1], Laura Heikkinen[1,2], Gilberto Fisone[1] and Christian Broberger[1,2,*]*

[1]Department of Neuroscience, Biomedicum B:4, Karolinska Institutet, Solnavägen 9, 171 65 Stockholm, Sweden

[2]Department of Biochemistry and Biophysics, Stockholm University, Svante Arrhenius väg 16C, 106 91 Stockholm, Sweden

[¶]Current address: Division of Biology and Biological Engineering 156-29, Tianqiao and Chrissy Chen Institute for Neuroscience, California Institute of Technology, Pasadena, CA 91125, USA

*Correspondence: stefanos.stagkourakis@caltech.edu, christian.broberger@dbb.su.se

Acknowledgments

Members of the Broberger laboratory are thanked for discussion during the preparation of this manuscript. This study was made possible by a European Research Council starting grant (ENDOSWITCH 261286), the Swedish Research Council (2018-02480), the Strategic Research Program in Diabetes at Karolinska Institutet, *Hjärnfonden* (the Swedish Brain Foundation), Novo Nordisk Fonden, Wenner-Gren Foundation funding, and internal funds from Karolinska Institutet.

Author contributions

S.S. and C.B. conceived the study and wrote the manuscript. S.S. designed, performed, and analyzed experiments. P.W., G.S., G.F., and C.B.designed experiments. P.W., G.S., S.K., K.Z., and L.H performed experiments. All authors reviewed the manuscript.

Competing interests

The authors declare no competing financial interests.

33 ## Graphical abstract

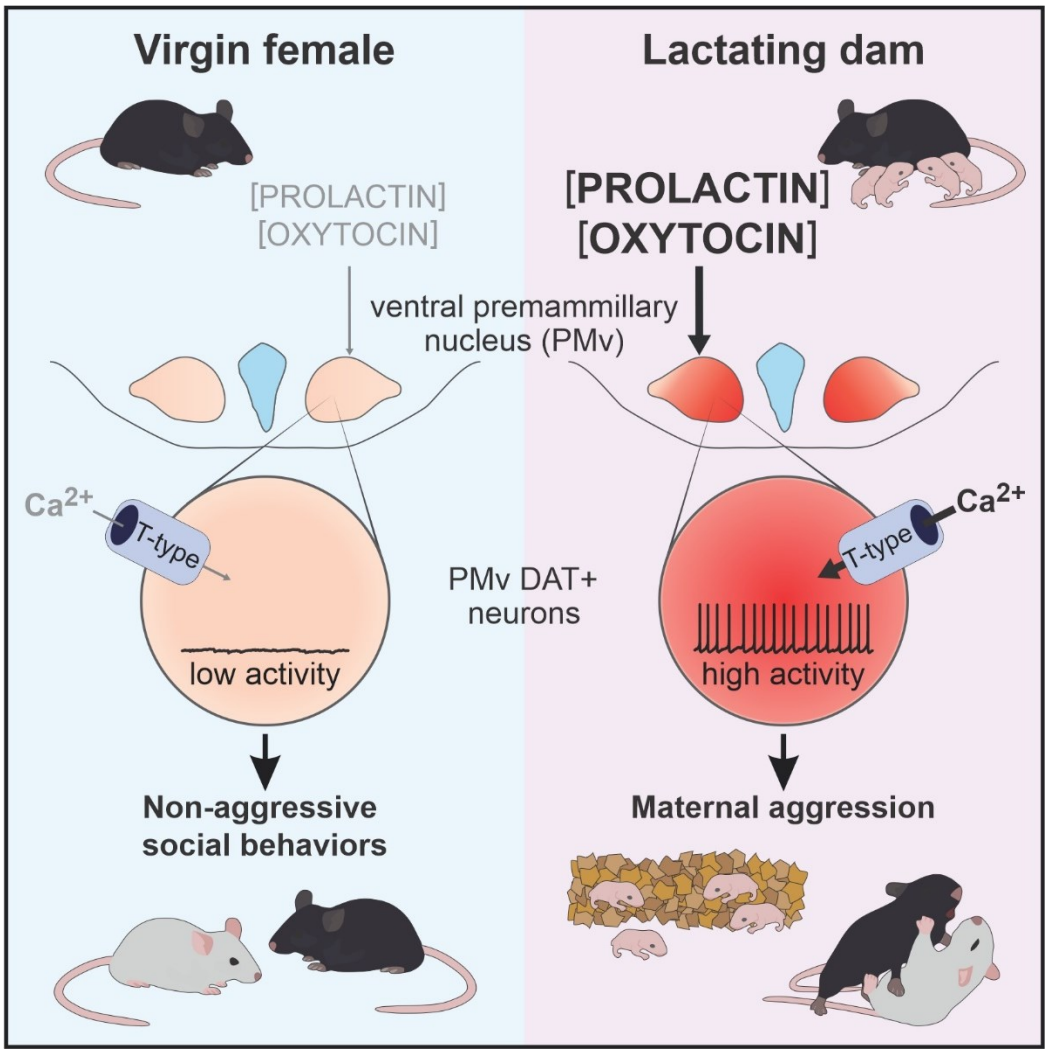

47

48 ## In Brief

49 Maternal hormones activate a subset of hypothalamic “aggression neurons”, which are required for
50 the transient expression of maternal aggression during lactation.

51

52 ## Highlights

53 - Quiescent PMv^{DAT} neurons in female mice become hyperexcitable in lactating dams.
54 - Manipulation of PMv^{DAT} cell activity bidirectionally regulates maternal aggression.
55 - The maternal hormones prolactin and oxytocin excite PMv^{DAT} cells.
56 - Activation of PMv^{DAT} neurons impairs the expression of non-aggression-related behavioral
57 programs.

Summary

Aggression - a sexually dimorphic behavior, is prevalent in males and typically absent in virgin females. Following parturition, however, the transient expression of aggression in adult females ensures the pups' defense from predators and infanticide. While maternal hormones are known to elicit nursing, whether they play a role in the expression of maternal aggression remains unknown. Here we show that a molecularly defined subset of ventral premammillary (PMv^{DAT}) neurons, instrumental for intermale aggression, switch into a hyperexcitable state during lactation. We identify that the maternal hormones prolactin and oxytocin excite these cells, an effect mediated through T-type Ca^{2+} channels. Optogenetic manipulation or genetic ablation of PMv^{DAT} neurons profoundly affects maternal aggression, while activation of these neurons impairs the expression of non-aggression-related behaviors. This work identifies a monomorphic neural substrate that incorporates hormonal cues to enable the transient expression of a dormant behavioral program in adult females.

Introduction

Aggression is a near-ubiquitous adaptive behavior in animals and man that serves multiple purposes and takes several forms, depending on agent and context (*1-8*). Intermale aggression is the most prevalent form of aggression found in nature, serving to establish intermale hierarchy and, consequently, access to resources and mating opportunities. In contrast, aggressive encounters in female mammals are mostly absent, with some notable exceptions (*9-11*). Female interactions with conspecifics, however, change dramatically after pregnancy and parturition, when lactating dams typically exhibit profound aggressive behavior towards conspecifics of both sexes (*12*). Indeed, maternal aggression is as indelible as other components of maternal behavior, such as nursing and nest-building. But this dramatic – yet reversible – phenotypical metamorphosis also presents a neurobiological enigma, specifically: How does the brain reconfigure to transiently enable the expression of a behavior that is otherwise outside of the animal's repertoire? The brain loci and mechanisms underlying maternal aggression are largely unknown (*13*), and the signals that drive this transition, alongside their site of action, remain ambiguous (*14*). Importantly, it remains unknown whether the neural modules that lead to the expression of aggression are shared between the two sexes, or exhibit sexual dimorphism. Finally, a question that stands out is whether brain nodes that elicit certain maternal behaviors facilitate or impair the expression of other maternal behaviors. Addressing this question would suggest a principle for the neural encoding of maternal behaviors, in *general* vs. *specialized* behavioral repertoire-eliciting nuclei.

Here we shed light on the above questions by focusing on the ventral premammillary nucleus (PMv), a node extending within the caudal two-thirds of the classically delineated "hypothalamic attack area" (*15*), and which has been recently implicated in social behavior (*16, 17*) and intermale aggression (*18-21*). This nucleus receives dense inputs from areas associated with sensory processing (*22*) and projects (*23*) to nuclei associated with social behavior (*24-27*), aggression (*19, 28-30*), and reward (*20, 31-34*). Within the PMv, a subset of glutamatergic cells that express the dopamine transporter (PMv^{DAT} neurons) has been specifically implicated in male agonistic behaviors (*18, 20, 21*).

Here we identify PMv^{DAT} cells as quiescent in the virgin female mouse brain, with a dramatic switch in their excitability during motherhood – excited by the hormones that surge during nursing and which facilitate the expression of maternal care. Specifically, prolactin (Prl) leads to excitatory pre- and post-synaptic changes, an effect also mimicked by another maternal hormone – oxytocin (OT). Optogenetic control of these neurons provides a bidirectional handle on maternal aggression, while partial genetic ablation hinders the expression of the behavior. Finally, activation of PMv^{DAT} neurons during a maternal care paradigm impairs the expression of pup retrieval and nursing, suggestive of a specialized role of PMv cells in eliciting a dedicated behavioral expression.

105 The present study suggests how the sex-specific expression of an adaptive behavior can result
106 from state-dependent tuning of neuronal excitability.
107

108 ## Results

109 **Low *vs* high baseline activity of PMv^{DAT} cells in virgin *vs* postpartum females**

110 While maternal aggression is widespread in the animal kingdom, recent studies suggest a high
111 degree of inter-individual variability in the expression of aggressive behavior (*20, 34, 35*). Previous
112 work has also shown that a number of variables impact on the expression of maternal aggression,
113 including litter size (*36*), pup presence (*37*), the intruder's sex (*38*) and behavior (*39*). To control for
114 these factors, we used a three consecutive day (p3-p5) resident-intruder (RI) paradigm to screen
115 lactating dams for aggressive behavior, using C57 or BALB/c juvenile female virgin mice (p40-50) as
116 intruders and restricting litter size to four to six pups *post partum* (Figure 1A). Under this paradigm,
117 42% of multiparous lactating dams expressed maternal aggression (Figure 1A), with increased
118 duration and decreased latency upon repeated experience in aggressive encounters (Figure 1B),
119 similar to what is observed in intermale aggression using the same paradigm (*20, 34, 40*).

120 A subpopulation of male laboratory rodents have consistently been shown to be non-aggressive
121 in the RI paradigm (*20, 34, 40*). Strikingly, PMv^{DAT} neurons in male non-aggressor mice are
122 significantly less electrically excitable than in aggressors (*41*). This observation prompted the question
123 if a similar phenotype-correlated electrical profile could be identified in lactating (aggressive) mice,
124 *vs*. virgin female mice (*42, 43*) who are non-aggressive. Brain slice whole-cell patch-clamp recordings
125 were performed on PMv^{DAT} cells, which were filled with 0.2% Neurobiotin for post-recording
126 identification (Figure 1E, F). Notably, PMv^{DAT} cells from lactating dams were more depolarized
127 compared to cells from virgin females (Figure 1G), exhibiting significantly higher firing frequency
128 (Figure 1H, Table S1) and a more depolarized resting membrane potential (Figure 1I, Table S1).

129 PMv neurons have been reported to activate in conjunction with an aggressive encounter in
130 lactating rat dams (*44*). To determine if this includes the PMv^{DAT} neurons, we examined c-Fos
131 immunoreactivity. Both the total number of c-Fos^{+} neurons, and the proportion of DAT^{+} cells
132 containing c-Fos^{+} immunoreactivity, were increased following the expression of maternal aggression
133 (Figure 1C, D, Table S1).

134 Having established that PMv^{DAT} neurons are in a hyperexcitable state in lactating dams compared
135 to the non-aggressive virgin female mouse, we next performed activation, inactivation and deletion of
136 these cells in order to investigate the effect of such manipulations *in vivo* on the expression of maternal
137 aggression. Genetic modifications were introduced into PMv^{DAT} neurons by stereotactic injection of
138 Cre-dependent constructs within an AAV vector.
139
140

141 **Bidirectional control of maternal aggression through PMv^{DAT} neurons**

142 PMv^{DAT} neurons in lactating dams were transduced with ChR2 (Figure 2B) and baseline behavior
143 was recorded in trials that were characterized by close investigation, but rare expressions of
144 aggression against male and female conspecifics (Figure 2A). Optogenetic stimulation resulted in
145 significantly prolonged attack bouts appearing within seconds of initiation of photostimulation (Figure
146 2C-E, Video S1, Table S1).

147 To determine the behavioral effect of inhibition of the PMv^{DAT} population, juvenile female intruders
148 were used to facilitate high levels of maternal aggression in baseline conditions(*38, 45*) (Figure 2F).
149 Indeed, under control conditions, lactating dams (Figure 2G) frequently engaged in sustained attacks.
150 However, application of optogenetic inhibition in these mice was followed by decreased attack bout
151 duration and delayed initiation of subsequent attack episodes (Figure 2H-J, Table S1).

152 Lastly, genetic deletion of the PMv^{DAT} neurons in lactating dams (Figure 2K, L) – sparing
153 neighboring DAT neuron populations (Figure S1A, B and Table S1) – dramatically decreased the
154 attack frequency and duration and increased latency to attack (Figure 2M-O, Table S1). Together,
155 these experiments establish a causal role for PMv^{DAT} neurons in the expression of maternal
156 aggression.

157

158 **Maternal hormones excite PMv^{DAT} neurons**

159 Endocrine hallmarks of the *post partum* female include a surge in the serum levels of specific
160 hormones (*46-50*). Among these hormones, the most well-documented maternal functions are served
161 by Prl (*51*), which rises in late pregnancy and remains elevated after birth in rodents (*52-54*),
162 facilitating maternal pup care behavior and offspring survival (*55-57*). OT which shows similar
163 dynamics, plays a parallel and complementary role in the mother's care for offspring (*58-61*). We next
164 explored if these maternal hormones can affect the activity of PMv^{DAT} neurons that the data above
165 implicate in puerperal aggression.

166 Serum levels of Prl were found ten-fold higher in lactating mouse dams compared to virgin females
167 at any point across the estrous cycle (Figure 3A, Table S1), in agreement with earlier literature (*62*).
168 We next determined if this difference in circulating Prl corresponds to differential Prl receptor (Prl-R)
169 activation in the PMv of virgin *vs* lactating female mice. Indeed, phosphorylation of the Signal
170 Transducer and Activator of Transcription 5 (pSTAT5), a key and sensitive downstream mediator of
171 Prl-R activation (*63-74*), was significantly elevated in PMv^{DAT} neurons in lactating females (Figure 3B-
172 D, Table S1). These findings prompted the question of whether PMv^{DAT} cells can be directly
173 modulated by Prl.

174 Application of Prl to PMv^{DAT} neurons during *in vitro* patch clamp recording yielded several
175 electrophysiological changes, which can increase the excitability and output of these cells. Firstly, a
176 prominent and reversible depolarization, paralleled by increased discharge frequency, was seen
177 (Figure 3E, Table S1), similar to observations from genetically unidentified PMv neurons (*75*).

178 Secondly, action potential duration was significantly prolonged (Figure 3F, Table S1), a change that
179 can increase neurotransmitter output by over a magnitude (*76*). Thirdly, the capacity for and strength
180 of post-inhibitory rebound were augmented (Figure 3G, Table S1), key features of PMv^{DAT} neurons
181 and implicated in their propensity for regenerative discharge (*20*). The post-synaptic Prl-induced
182 current in PMv^{DAT} cells consisted of a low- and a high-voltage component (Figure 3H, Table S1).
183 Application of the selective T-type low-threshold Ca^{2+} current blocker, ML-218, abolished the low-
184 voltage component (Figure 3I, Table S1). Lastly we tested whether blocking the T-type Ca^{2+} channels
185 impaired the post-inhibitory rebound, and the Prl induced potentiation of rebound excitation. Indeed,
186 ML218 abolished the post-inhibitory rebound current and effect of Prl at below firing threshold
187 membrane potential (data not shown).

188 Interestingly, the application of Prl also affected synaptic input into PMv^{DAT} neurons, with an
189 increase of both spontaneous excitatory (Figure 3J, Table S1) and inhibitory post-synaptic currents
190 (data not shown). A likely source of the increased excitatory synaptic currents is recurrent axon
191 collaterals, as the glutamatergic PMv^{DAT} population is densely interconnected (*20*). These data reveal
192 a wide repertoire of Prl actions on the membrane properties of PMv^{DAT} neurons that together converge
193 to increase excitability.

194 Oxytocin, beyond its role in milk ejection (*77-79*), is most commonly discussed as an agent of
195 maternal care and social bonding (*80, 81*). Previous studies have, however, also correlated increased
196 serum OT levels to maternal aggression (*82-84*). Yet, the neural substrates underlying this effect
197 remain unknown. Immunofluorescence staining of the PMv identified close appositions between OT
198 positive fibers and PMv^{DAT} cell somata (Figure 3K). This finding, and the presence of OT receptors
199 (OT-R's) in the PMv (*85*), led us to evaluate the responsiveness of PMv^{DAT} neurons to OT. Application
200 of OT led to a reversible depolarization of PMv^{DAT} neurons (Figure 3L, Table S1), similar to the effect
201 of Prl (as above), as did application of the selective OT-R agonist, TGOT (*86, 87*)(Figure 3M, Table
202 S1). However, the effect of OT persisted also in the presence of an OT-R antagonist (vasotocin
203 [$d(CH2)_5^1$, $Tyr(Me)^2$, Thr^4, Orn^8, des-Gly NH_2^9]), indicating that vasopressin receptors (*88-93*)
204 contribute to the peptide's action on PMv^{DAT} neurons (Figure 3M, Table S1). The OT effect depended
205 on a post-synaptic depolarization, composed of low- and high-voltage components similar to the Prl-
206 induced current (Figure 3N, Table S1).

207 To investigate whether maternal hormones acting in the PMv are sufficient to trigger aggression
208 in an inherently non-aggressive female, we performed a 28-day localized application of Prl, OT, or
209 both peptide hormones (co-administration) unilaterally into the nucleus of virgin female adult mice.
210 Two weeks after implantation we performed a panel of tests, to investigate changes in aggressive
211 and/or maternal behavior, as well as other behavioral features. No attacks or changes in the degree
212 of close investigation were observed in the RI test (Figure S2A, B and Table S1). Notably, however,
213 local co-administration of maternal hormones in PMv decreased sociability in the group (Figure S2C,

Table S1) and, importantly, impaired maternal behavior (Figure S2D, Table S1). Modest changes in locomotion, but not anxiety parameters, were identified (Figure S2E-F, Table S1).

Together these experiments identify that PMv-targetted application of maternal hormones in non-lactating females does not lead to the expression of aggression, suggestive of necessary upstream and/or downstream changes implemented in the brains of lactating dams. However, of interest are the observations that administration of maternal hormones in the PMv of non-lactating mice leads to a decrease in sociability (Figure S2C) and impairs performance in the pup retrieval test (Figure S2D).

Activation of PMv^{DAT} neurons impairs maternal care

Aggression in dams is part of a behavioral program that turns on at parturition and declines by weaning (*38, 94*). This program includes a coincident initiation of pup care – such as nursing, grooming and crouching, and maternal aggression – aimed to inflict injury and deter infanticidal conspecifics or predators from attacking the pups (*94*). In the final experiment, we tested whether *pup care* and *maternal aggression* can be triggered by common anatomical substrates – such as PMv, or whether activation of defined brain loci/circuitry leads to the execution of dedicated/non-overlapping behavioral programs at the expense of other behaviors.

To investigate this issue, we tested the effect of optogenetic activation of PMv^{DAT} neurons in the absence of a conspecific – during a pup retrieval test (*95, 96*). The pup retrieval test was performed in lactating dams expressing ChR2 or eYFP in PMv^{DAT} neurons (Figure 4A, B). Control (eYFP-expressing) dams retrieved all pups within a minute of the task initiation during photostimulation (Figure 4B, D, E, Video S2, Table S1). In contrast, photostimulated ChR2-expressing dams exhibited severely impaired pup-retrieval behavior and in many cases, failed to retrieve any pups over the maximum test period of three minutes (Figure 4B-E, Video S3, Table S1). No aggression towards the pups was observed in any of the trials.

These data suggest that activation of these neurons promotes a specialized behavioral program – the one of maternal aggression, at the expense of other maternal behaviors. This is illustrated in the data discussed here, where even in the absence of a competing intruder stimulus, normal nursing behavior is inhibited. It is likely that PMv^{DAT} neuron activity serves multiple functions, facilitating the expression of maternal aggression and inhibiting the expression of antagonistic behaviors.

Discussion

The data presented here, identify a PMv neuron subpopulation in the hypothalamus as a key node in orchestrating maternal aggression but not maternal care. The identification of the node's activation following a maternal aggression episode, together with the finding that maternal hormones act upon the PMv^{DAT} cells in an excitatory manner, provide a long-missing link in the neurobiological understanding of aggressive behavior in females.

These data suggest that the sexual dimorphism in the expression of aggressive behavior likely does not stem from a fundamentally different wiring between the male and the female brain. Rather, a common framework for aggression exists across the two sexes that can be recruited for adaptive purposes (e.g. to establish social rank among males or to secure the survival of pups in post-partum females). It remains a conundrum how this ultimately yields a different motor expression – pattern of behavior – and what the underlying switch consists of.

It is important to note here that PMv^{DAT} neurons have been associated with a number of social behaviors in male mice (*18-20*), primarily with aggressive behavior. Together these findings suggest that at least part of the aggression circuit active in males, is recruited via the increase of maternal hormones in the serum of lactating females. Of particular interest is the observation that the increase in serum Prl likely leads to activation of numerous nuclei in the CNS to induce the collective behavioral repertoire known as maternal behavior, with classically defined adaptations including energy homeostasis (*97*), nursing behavior (*57*), and aggression (*98-100*). While recent work has provided evidence for the role of Prl-R activation in the medial preoptic area of the hypothalamus specifically in nursing behavior (*57*), here we suggest that Prl-R mediated activation of the PMv and the downstream circuit recruits the maternal aggression behavioral repertoire while suppressing competing behavioral programs.

Finally, application of maternal hormones locally in the PMv of adult females was shown to be insufficient to induce aggressive behavior in female mice, indicative of necessary circuit adaptations upstream of the PMv. Future work is needed in order to further identify the necessary sites of action of maternal hormones, whose activation enables the expression of aggression in females.

References

1. D. Maestripieri, Costs and Benefits of Maternal Aggression in Lactating Female Rhesus Macaques. *Primates; journal of primatology* **35**, 443-453 (1994).
2. J. P. Kent, Maternal Aggression and Interindividual Distance in the Broody Hen (Gallus-Gallus). *Behav Process* **27**, 37-44 (1992).
3. A. Troisi, F. R. Damato, A. Carnera, L. Trinca, Maternal Aggression by Lactating Group-Living Japanese Macaque Females. *Hormones and behavior* **22**, 444-452 (1988).
4. B. Olivier *et al.*, Maternal Aggression in Rats. *Aggressive Behav* **11**, 169-169 (1985).
5. E. R. Stockman, Aggressive Experience and Maternal Aggression in the Mongolian Gerbil. *Physiology & behavior* **30**, 319-321 (1983).
6. H. I. Siegel, A. L. Giordano, C. M. Mallafre, J. S. Rosenblatt, Maternal Aggression in Hamsters - Effects of Stage of Lactation, Presence of Pups, and Repeated Testing. *Hormones and behavior* **17**, 86-93 (1983).
7. R. D. Stjohn, P. A. Corning, Maternal Aggression in Mice. *Behavioral biology* **9**, 635-639 (1973).
8. M. H. Figler, G. S. Blank, H. V. S. Peeke, Maternal aggression and post-hatch care in red swamp crayfish, Procambarus clarkii (Girard): The influences of presence of offspring, fostering, and maternal molting. *Mar Freshw Behav Phy* **30**, 173-194 (1997).
9. K. Hashikawa *et al.*, Esr1(+) cells in the ventromedial hypothalamus control female aggression. *Nature neuroscience* **20**, 1580-1590 (2017).
10. N. M. Rendon, G. E. Demas, Bi-directional actions of dehydroepiandrosterone and aggression in female Siberian hamsters. *Journal of experimental zoology. Part A, Ecological genetics and physiology* **325**, 116-121 (2016).
11. L. E. Been, K. M. Moore, B. C. Kennedy, R. L. Meisel, Metabotropic Glutamate Receptor and Fragile X Signaling in a Female Model of Escalated Aggression. *Biological psychiatry* **79**, 685-692 (2016).
12. J. S. Lonstein, S. C. Gammie, Sensory, hormonal, and neural control of maternal aggression in laboratory rodents. *Neuroscience and biobehavioral reviews* **26**, 869-888 (2002).
13. M. Liu, D. W. Kim, H. Zeng, D. J. Anderson, Make war not love: The neural substrate underlying a state-dependent switch in female social behavior. *Neuron* **110**, 841-856 e846 (2022).
14. T. Georgescu, Z. Khant Aung, D. R. Grattan, R. S. E. Brown, Prolactin-mediated restraint of maternal aggression in lactation. *Proceedings of the National Academy of Sciences of the United States of America* **119**, (2022).
15. M. R. Kruk *et al.*, Discriminant analysis of the localization of aggression-inducing electrode placements in the hypothalamus of male rats. *Brain research* **260**, 61-79 (1983).
16. J. C. Cavalcante, J. C. Bittencourt, C. F. Elias, Female odors stimulate CART neurons in the ventral premammillary nucleus of male rats. *Physiology & behavior* **88**, 160-166 (2006).
17. M. Yokosuka *et al.*, Female-soiled bedding induced Fos immunoreactivity in the ventral part of the premammillary nucleus (PMv) of the male mouse. *Physiology & behavior* **68**, 257-261 (1999).
18. M. E. Soden *et al.*, Genetic Isolation of Hypothalamic Neurons that Regulate Context-Specific Male Social Behavior. *Cell reports* **16**, 304-313 (2016).
19. D. Y. Lin *et al.*, Functional identification of an aggression locus in the mouse hypothalamus. *Nature* **470**, 221-+ (2011).
20. S. Stagkourakis *et al.*, A neural network for intermale aggression to establish social hierarchy. *Nature neuroscience* **21**, 834-+ (2018).
21. A. X. Chen *et al.*, Specific Hypothalamic Neurons Required for Sensing Conspecific Male Cues Relevant to Inter-male Aggression. *Neuron*, (2020).
22. J. C. Cavalcante, J. C. Bittencourt, C. F. Elias, Distribution of the neuronal inputs to the ventral premammillary nucleus of male and female rats. *Brain research* **1582**, 77-90 (2014).
23. N. S. Canteras, R. B. Simerly, L. W. Swanson, Projections of the Ventral Premammillary Nucleus. *Journal of Comparative Neurology* **324**, 195-212 (1992).

24. M. M. Sanchez, F. Aguado, F. Sancheztoscano, D. Saphier, Effects of Prolonged Social-Isolation on Responses of Neurons in the Bed Nucleus of the Stria Terminalis, Preoptic Area, and Hypothalamic Paraventricular Nucleus to Stimulation of the Medial Amygdala. *Psychoneuroendocrinology* **20**, 525-541 (1995).
25. N. Duque-Wilckens, M. Steinman, V. Grinevich, B. Trainor, The Role of Oxytocin Neurons in the Bed Nucleus of the Stria Terminalis in Mediating Social Withdrawal. *Biological psychiatry* **81**, S44-S45 (2017).
26. K. Lei, B. S. Cushing, S. Musatov, S. Ogawa, K. M. Kramer, Estrogen Receptor-alpha in the Bed Nucleus of the Stria Terminalis Regulates Social Affiliation in Male Prairie Voles (Microtus ochrogaster). *PloS one* **5**, (2010).
27. A. M. Jasnow, M. Davis, K. L. Huhman, Involvement of central amygdalar and bed nucleus of the stria terminalis corticotropin-releasing factor in behavioral responses to social defeat. *Behavioral neuroscience* **118**, 1052-1061 (2004).
28. D. J. Albert, M. L. Walsh, B. B. Gorzalka, S. Mendelson, C. Zalys, Intermale Social Aggression - Suppression by Medial Preoptic Area Lesions. *Physiology & behavior* **38**, 169-173 (1986).
29. J. S. Rosenblatt, S. Hazelwood, J. Poole, Maternal behavior in male rats: Effects of medial preoptic area lesions and presence of maternal aggression. *Hormones and behavior* **30**, 201-215 (1996).
30. N. Scott, M. Prigge, O. Yizhar, T. Kimchi, A sexually dimorphic hypothalamic circuit controls maternal care and oxytocin secretion. *Nature* **525**, 519-+ (2015).
31. H. Vogel *et al.*, GLP-1 and estrogen conjugate acts in the supramammillary nucleus to reduce food-reward and body weight. *Neuropharmacology* **110**, 396-406 (2016).
32. R. Shin, S. Ikemoto, Administration of the GABA(A) receptor antagonist picrotoxin into rat supramammillary nucleus induces c-Fos in reward-related brain structures. Supramammillary picrotoxin and c-Fos expression. *BMC neuroscience* **11**, (2010).
33. S. Ikemoto, B. M. Witkin, A. Zangen, R. A. Wise, Rewarding effects of AMPA administration into the supramammillary or posterior hypothalamic nuclei but not the ventral tegmental area. *Journal of Neuroscience* **24**, 5758-5765 (2004).
34. S. A. Golden *et al.*, Basal forebrain projections to the lateral habenula modulate aggression reward. *Nature* **534**, 688-692 (2016).
35. S. A. Golden *et al.*, Compulsive Addiction-like Aggressive Behavior in Mice. *Biological psychiatry* **82**, 239-248 (2017).
36. D. Maestripieri, E. Alleva, Maternal Aggression and Litter Size in the Female House Mouse. *Ethology* **84**, 27-34 (1990).
37. K. J. Flannelly, E. D. Kemble, The Effect of Pup Presence and Intruder Behavior on Maternal Aggression in Rats. *B Psychonomic Soc* **25**, 133-135 (1987).
38. M. Haney, J. F. Debold, K. A. Miczek, Maternal Aggression in Mice and Rats Towards Male and Female Conspecifics. *Aggressive Behav* **15**, 443-453 (1989).
39. J. Mos, B. Olivier, R. Vanoorschot, Maternal Aggression Towards Different Sized Male Opponents - Effect of Chlordiazepoxide Treatment of the Mothers and D-Amphetamine Treatment of the Intruders. *Pharmacol Biochem Be* **26**, 577-584 (1987).
40. S. Stagkourakis, G. Spigolon, G. Liu, D. J. Anderson, Experience-dependent plasticity in an innate social behavior is mediated by hypothalamic LTP. *Proceedings of the National Academy of Sciences of the United States of America* **117**, 25789-25799 (2020).
41. S. Stagkourakis *et al.*, A neural network for intermale aggression to establish social hierarchy. *Nature neuroscience* **21**, 834-842 (2018).
42. S. M. Howard, R. Gandelman, C. Rosenthal, Isolation Potentiates the Aggression-Activating Property of Testosterone in Female Mice. *Physiology & behavior* **26**, 971-972 (1981).
43. M. S. Barkley, B. D. Goldman, Testosterone-Induced Aggression in Adult Female Mice. *Hormones and behavior* **9**, 76-84 (1977).
44. S. C. Motta *et al.*, Ventral premammillary nucleus as a critical sensory relay to the maternal aggression network. *Proceedings of the National Academy of Sciences of the United States of America* **110**, 14438-14443 (2013).
45. K. J. Flannelly, L. Flannelly, Opponents Size Influences Maternal Aggression. *Psychological reports* **57**, 883-886 (1985).

46. M. D. M. Hallak, J. W. Hotra, Maternal serum hormone concentrations in Long-Evans rats. *J Trace Microprobe T* **21**, 103-110 (2003).
47. C. M. Dwyer, A. B. Lawrence, Induction of maternal behaviour in non-pregnant, hormone-primed ewes. *Anim Sci* **65**, 403-408 (1997).
48. J. H. Duenhoelter, Maternal Hormone Measurements. *Jama-J Am Med Assoc* **248**, 1109-1109 (1982).
49. C. D. Hansult, S. Kessler, Role of Hormones in Maternal Aggression and Infant Care. *Behavior genetics* **7**, 65-66 (1977).
50. M. X. Zarrow, V. H. Denenberg, R. Gandelman, Prolactin - Is It an Essential Hormone for Maternal Behavior in Mammal. *Hormones and behavior* **2**, 343-+ (1971).
51. O. Riddle, Prolactin in Vertebrate Function and Organization. *Jnci-J Natl Cancer I* **31**, 1039-+ (1963).
52. M. Lhermite, Gonadotropin and Prolactin Function during Pregnancy and Postpartum. *Rev Fr Gynecol Obste* **71**, 159-165 (1976).
53. H. Moltz, R. Levin, M. Leon, Prolactin in Postpartum Rat - Synthesis and Release in Absence of Suckling Stimulation. *Science* **163**, 1084-& (1969).
54. J. W. Riesen, Saiduddi.S, W. E. Graves, W. J. Tyler, L. E. Casida, Pituitary Prolactin Activity in Postpartum Dairy Cows. *Journal of animal science* **25**, 929-& (1966).
55. M. Numan, H. Moltz, M. Leon, Interference with Prolactin Release and Maternal Behavior of Female Rats. *Hormones and behavior* **3**, 29-& (1972).
56. R. S. Bridges, B. D. Goldman, L. P. Bryant, Serum Prolactin Concentrations and Initiation of Maternal-Behavior in Rat. *Hormones and behavior* **5**, 219-226 (1974).
57. R. S. E. Brown *et al.*, Prolactin action in the medial preoptic area is necessary for postpartum maternal nursing behavior. *Proceedings of the National Academy of Sciences of the United States of America* **114**, 10779-10784 (2017).
58. C. A. Pedersen, A. J. Prange, Jr., Induction of maternal behavior in virgin rats after intracerebroventricular administration of oxytocin. *Proceedings of the National Academy of Sciences of the United States of America* **76**, 6661-6665 (1979).
59. C. A. Pedersen, J. A. Ascher, Y. L. Monroe, A. J. Prange, Jr., Oxytocin induces maternal behavior in virgin female rats. *Science* **216**, 648-650 (1982).
60. A. Watarai *et al.*, The blockade of oxytocin receptors in the paraventricular thalamus reduces maternal crouching behavior over pups in lactating mice. *Neuroscience letters* **720**, 134761 (2020).
61. F. Champagne, J. Diorio, S. Sharma, M. J. Meaney, Naturally occurring variations in maternal behavior in the rat are associated with differences in estrogen-inducible central oxytocin receptors. *Proceedings of the National Academy of Sciences of the United States of America* **98**, 12736-12741 (2001).
62. A. Guillou *et al.*, Assessment of lactotroph axis functionality in mice: longitudinal monitoring of PRL secretion by ultrasensitive-ELISA. *Endocrinology* **156**, 1924-1930 (2015).
63. F. Gouilleux, H. Wakao, M. Mundt, B. Groner, Prolactin Induces Phosphorylation of Tyr694 of Stat5 (Mgf), a Prerequisite for DNA-Binding and Induction of Transcription. *Embo Journal* **13**, 4361-4369 (1994).
64. L. DaSilva *et al.*, Prolactin recruits STAT1, STAT3 and STAT5 independent of conserved receptor tyrosines TYR402, TYR479, TYR515 and TYR580. *Molecular and cellular endocrinology* **117**, 131-140 (1996).
65. S. Ali, S. Ali, Prolactin receptor regulates Stat5 tyrosine phosphorylation and nuclear translocation by two separate pathways. *Journal of Biological Chemistry* **273**, 7709-7716 (1998).
66. A. Lerant, B. Kanyicska, M. E. Freeman, Nuclear translocation of STAT5 and increased expression of Fos related antigens (FRAs) in hypothalamic dopaminergic neurons after prolactin administration. *Brain research* **904**, 259-269 (2001).
67. J. L. Brockman, L. A. Schuler, Prolactin signals via Stat5 and Oct-1 to the proximal cyclin D1 promoter. *Molecular and cellular endocrinology* **239**, 45-53 (2005).
68. B. J. Cave *et al.*, Prolactin-induced activation of STAT5 within the hypothalamic arcuate nucleus. *Neuroreport* **16**, 1423-1426 (2005).

69. S. Jaroenporn, K. Nagaoka, R. Ohta, G. Watanabe, K. Taya, Prolactin induces phosphorylation of the STAT5 in adrenal glands of Hatano rats during stress. *Life sciences* **85**, 172-177 (2009).
70. J. D. Buntin, L. Buntin, Increased STAT5 signaling in the ring dove brain in response to prolactin administration and spontaneous elevations in prolactin during the breeding cycle. *General and comparative endocrinology* **200**, 1-9 (2014).
71. R. S. E. Brown, I. C. Kokay, A. E. Herbison, D. R. Grattan, Distribution of Prolactin-Responsive Neurons in the Mouse Forebrain. *Journal of Comparative Neurology* **518**, 92-102 (2010).
72. R. A. Augustine *et al.*, Prolactin regulation of oxytocin neurone activity in pregnancy and lactation. *J Physiol-London* **595**, 3591-3605 (2017).
73. R. S. E. Brown, A. E. Herbison, D. R. Grattan, Effects of Prolactin and Lactation on A15 Dopamine Neurones in the Rostral Preoptic Area of Female Mice. *Journal of neuroendocrinology* **27**, 708-717 (2015).
74. R. S. E. Brown, R. Piet, A. E. Herbison, D. R. Grattan, Differential Actions of Prolactin on Electrical Activity and Intracellular Signal Transduction in Hypothalamic Neurons. *Endocrinology* **153**, 2375-2384 (2012).
75. M. A. Silveira *et al.*, Acute effects of somatomammotropin hormones on neuronal components of the hypothalamic-pituitary-gonadal axis. *Brain research* **1714**, 210-217 (2019).
76. B. L. Sabatini, W. G. Regehr, Control of neurotransmitter release by presynaptic waveform at the granule cell to Purkinje cell synapse. *The Journal of neuroscience : the official journal of the Society for Neuroscience* **17**, 3425-3435 (1997).
77. A. Kamikawa, J. Seko, Physiological and pharmacological evaluation of oxytocin-induced milk ejection in mice. *Experimental animals* **69**, 345-353 (2020).
78. Y. F. Wang, G. I. Hatton, Milk ejection burst-like electrical activity evoked in supraoptic oxytocin neurons in slices from lactating rats. *Journal of neurophysiology* **91**, 2312-2321 (2004).
79. J. D. Donker, J. H. Koshi, W. E. Petersen, The effect of exogenous oxytocin in blocking the normal relationship between endogenous oxytocic substance and the milk ejection phenomenon. *Science* **119**, 67-68 (1954).
80. C. Finkenwirth, E. Martins, T. Deschner, J. M. Burkart, Oxytocin is associated with infant-care behavior and motivation in cooperatively breeding marmoset monkeys. *Hormones and behavior* **80**, 10-18 (2016).
81. H. E. Ross, L. J. Young, Oxytocin and the neural mechanisms regulating social cognition and affiliative behavior. *Frontiers in neuroendocrinology* **30**, 534-547 (2009).
82. J. P. Stohn *et al.*, Increased aggression and lack of maternal behavior in Dio3-deficient mice are associated with abnormalities in oxytocin and vasopressin systems. *Genes Brain and Behavior* **17**, 23-35 (2018).
83. O. J. Bosch, Maternal aggression in rodents: brain oxytocin and vasopressin mediate pup defence. *Philos T R Soc B* **368**, (2013).
84. O. J. Bosch, S. L. Meddle, D. I. Beiderbeck, A. J. Douglas, I. D. Neumann, Brain oxytocin correlates with maternal aggression: Link to anxiety. *Journal of Neuroscience* **25**, 6807-6815 (2005).
85. P. Kremarik, M. J. Freund-Mercier, M. E. Stoeckel, Oxytocin and vasopressin binding sites in the hypothalamus of the rat: histoautoradiographic detection. *Brain research bulletin* **36**, 195-203 (1995).
86. M. Zaninetti, M. Raggenbass, Oxytocin receptor agonists enhance inhibitory synaptic transmission in the rat hippocampus by activating interneurons in stratum pyramidale. *The European journal of neuroscience* **12**, 3975-3984 (2000).
87. J. Elands, C. Barberis, S. Jard, [3H]-[Thr4,Gly7]OT: a highly selective ligand for central and peripheral OT receptors. *The American journal of physiology* **254**, E31-38 (1988).
88. J. Gruskos, A. Goldwaser, D. A. Guarracino, Competition of peptide hormone mimics with vasopressin and oxytocin for binding their target membrane receptors. *Abstr Pap Am Chem S* **244**, (2012).
89. M. Hibert *et al.*, Functional architecture of vasopressin/oxytocin receptors. *Journal of receptor and signal transduction research* **19**, 589-596 (1999).

90. H. H. Zingg, Vasopressin and oxytocin receptors. *Bailliere Clin Endoc* **10**, 75-96 (1996).
91. M. Manning, S. Stoev, W. Y. Chan, W. H. Sawyer, Receptor-Specific Antagonists of Vasopressin and Oxytocin - a Current Perspective. *Neurohypophysis : A Window on Brain Function* **689**, 219-232 (1993).
92. S. Jard, J. Elands, A. Schmidt, C. Barberis, Vasopressin and Oxytocin Receptors - an Overview. *Progress in Endocrinology 1988, Vol 1 and 2* **799**, 1183-1188 (1988).
93. P. J. Martin, H. O. Schild, Interaction of Oxytocin and Vasopressin with Tissue Receptors. *Biochemical pharmacology* **12**, 139-& (1963).
94. R. D. St John, P. A. Corning, Maternal aggression in mice. *Behavioral biology* **9**, 635-639 (1973).
95. A. Zimprich *et al.*, Assessing Sociability, Social Memory, and Pup Retrieval in Mice. *Current protocols in mouse biology* **7**, 287-305 (2017).
96. A. Bendesky *et al.*, The genetic basis of parental care evolution in monogamous mice. *Nature* **544**, 434-439 (2017).
97. S. R. Ladyman *et al.*, Prolactin receptors in Rip-cre cells, but not in AgRP neurones, are involved in energy homeostasis. *Journal of neuroendocrinology* **29**, (2017).
98. J. A. Barry *et al.*, Prolactin and aggression in women with fertility problems. *Journal of Obstetrics and Gynaecology* **34**, 605-610 (2014).
99. A. R. Consiglio, R. S. Bridges, Circulating prolactin, MPOA prolactin receptor expression and maternal aggression in lactating rats. *Behavioural brain research* **197**, 97-102 (2009).
100. P. E. Gleason, S. D. Michael, J. J. Christian, Prolactin-Induced Aggression in Female Peromyscus-Leucopus. *Behavioral and neural biology* **33**, 243-248 (1981).
101. M. I. Ekstrand *et al.*, Progressive parkinsonism in mice with respiratory-chain-deficient dopamine neurons. *Proceedings of the National Academy of Sciences of the United States of America* **104**, 1325-1330 (2007).
102. K. B. J. Franklin, G. Paxinos, *THE MOUSE BRAIN IN STEREOTACTIC COORDINATES*. (2008), vol. Third edition.
103. R. Behringer, M. Gertsenstein, K. V. Nagy, A. Nagy, Selecting Female Mice in Estrus and Checking Plugs. *Cold Spring Harb Protoc* **2016**, (2016).

518 ## Materials and methods

519 **Animals.** All animal experiments had received approval from the local ethical board, *Stockholms*
520 *Norra Djurförsöksetiska Nämnd*, and were performed in accordance with the European Communities
521 Council Directive of November 24, 1986 (86/609/EEC). Wild-type mice with C57BL/6J and BALB/c
522 background were used, in addition to previously generated C57BL/6J *Slc6a*^{Cre} (DAT-Cre) knock-
523 in(*101*) and floxed-tdTomato mice (The Jackson Laboratory, strain datasheet – 007909). Animals
524 were group-housed, up to five per cage, in a temperature (23°C) and humidity (55%) controlled
525 environment, in a 12h light, 12h dark cycle with *ad libitum* access to food and water. Cages were
526 changed on a weekly basis.
527 Adult female virgin, and lactating female mice used in experiments were single housed for a period
528 of two to four weeks, depending on the experimental design. Only multiparous lactating mice were
529 used in the experimental group of *lactating dams*, typically following their third or fourth parturition.
530
531 **Viral vectors.** For channelrhodopsin optogenetic studies animals were injected in the PMv with
532 400 nL of AAV5-EF1a-DIO-hChR2(H134R)-eYFP-WPRE-hGH (Addgene20298) 8.41 × 10^{12} genomic
533 copies per mL. For halorhodopsin-mediated neuronal silencing, animals were injected with 400 nL of
534 AAV5-EF1a-DIO-eNpHR3.0-eYFP-WPRE-hGH (Addgene26966) 7.02 × 10^{12} genomic copies per mL.
535 The control groups in optogenetic were injected with 400 nL of AAV5-EF1a-DIO-eYFP-WPRE-hGH
536 (Addgene27056) 5.82 × 10^{12} genomic copies per mL. The ChR2, eNpHR3 and eYFP AAV5 were
537 prepared by the University of Pennsylvania Vector Core. For targeted cell ablation of DAT^{+} PMv
538 neurons animals were injected in PMv with 300 nL of AAV5-flex-taCasp3-TEVp 2.9 × 10^{12} genomic
539 copies per mL, and the AAV was prepared by the viral vector core at the University of North Carolina.
540 Viral injections were performed bilaterally.
541
542 **Stereotactic surgery and viral gene transfer.** Adult DAT-Cre mice 5-8 months old (sexually
543 inexperienced) were stereotactically injected with a virus, and implanted with fiber implants when
544 purposed for *in vivo* optogenetic behavior experiments, and were individually housed for 2 weeks
545 post-surgery. Animals were anaesthetized with isoflurane (1–5%) and placed in a stereotactic frame
546 (David Kopf Instruments). Virus was injected into the PMv bilaterally using a pulled glass capillary
547 (World Precision Instruments) by nanolitre pressure injection at a flow rate of 50 nL per min (Micro4
548 controller, World Precision Instruments; Nanojector II, Drummond Scientific). Stereotactic injection
549 coordinates to target the PMv were obtained from the Paxinos and Franklin atlas (*102*) (Bregma: -
550 2.45 mm, midline ±0.6 mm, dorsal surface -5.5 mm). Ferrules and fiber-optic patch cords were
551 purchased from Thorlabs and Doric Lenses, respectively. The virus-injected animals were housed
552 individually during a 2-week recovery period, and then examined behaviorally and histologically.

553 In the case of the *lactating dams* group, sexually experienced female mice with prior maternal
554 experience were placed in a cage with a male mouse, and were checked for plugs in the morning
555 hours of the next four days (*103*). Following identification of plugs, female mice were single housed,
556 and surgeries were performed for AAV injections, and/or optic fiber implants. The surgical procedures
557 occurred within a week of plug identification. Female mice in which plug identification did not occur or
558 was ambiguous were excluded from the study.
559
560 **Optogenetics.** In optogenetic experiments, subjects were coupled via a ferrule patch cord to a
561 ferrule on the head of the mouse using a zirconia split sleeve (Doric Lenses). The optical fiber was
562 connected to a laser (447 nm for ChR2; 635 nm for eNpHR3; CNI-MLL-III-447-200-5-LED and CNI-
563 MLL-III-635-200-5-LED, CNI lasers 200 mW) via a fiber-optic rotary joint (FRJ_1x1_FC-FC, Doric
564 Lenses) to avoid twisting of the cable caused by the animal's movement. After a testing session, DAT-
565 Cre animals were uncoupled from the fiber-optic cable and returned to a housing room. The frequency
566 and duration of photostimulation were controlled using custom written LabView software. Laser power
567 was controlled by dialling an analogue knob on the power supply of the laser sources. Light power
568 was measured from the tip of the ferrule in the patch cord before being installed in the brain (the
569 ferrule-connector system) at different laser output settings, using an optical power and energy meter
570 and a photodiode power sensor (Thorlabs). Upon identification of the fiber placement coordinates in
571 brain tissue slides, irradiance (light intensity) was calculated using the brain tissue light transmission
572 calculator based on (http://www.stanford.edu/group/dlab/cgi-bin/graph/chart.php) using laser power
573 measured at the tip and the distance from the tip to the target brain region measured by histology.
574 Animals showing no detectable viral expression in the target region and/or ectopic fiber placement
575 were excluded from analysis. In some experiments, animals were photostimulated with a train of 473
576 nm light (20 Hz, 5 msec, 5 min) 45 min before perfusion in the absence of an intruder at an intensity
577 which had evoked a behavioral phenotype in the final testing session. Brain sections were
578 subsequently immunohistochemically labelled for c-Fos to identify optogenetically activated cells.
579
580 **Behavioral tests.** Behavioral tests were performed at 2h post-initiation of the light phase and 2h
581 prior to initiation of the dark phase. Mice were acclimated to the testing facility for 1 h prior to testing.
582 Behaviors were recorded using a digital video recording unit. Behavioral annotations were performed
583 manually, with conditions blinded to the experimenter performing the behavioral scoring.
584
585 **Resident-intruder (RI) test.** RI tests were initiated at 2 to 4 weeks post-surgery and repeated
586 weekly for 2 to 5 weeks. All dams used in the present study were multiparous and were used in
587 behavioral experiments during their third or fourth litter. Mouse cages were not cleaned for a minimum
588 of 3 days prior to the behavioral test. Intruders were individually introduced to a DAT-Cre mouse in a
589 testing session in a random order with respect to sex, with a 5 min interval between intruders. The

590 types of intruders were: juvenile females and adult females. Subjects involved in the RI test were
591 exposed to 3 experimental days of the test, resulting in multiple measurements per resident.
592
593 **ChR2-mediated activation in RI.** After the introduction of an intruder, a virus-injected animal was
594 recorded for 3 min to assess baseline behavior towards each intruder. The baseline recording was
595 followed by photostimulation trials (3 min in duration) with varying irradiance (intensity), stimulation
596 intervals, distance, orientation and recent behavior history between the two animals at the onset of
597 photostimulation. The AAV5-DIO-eYFP and AAV5-DIO-ChR2 injected experimental animals were
598 processed in random order.
599
600 **eNpHR3-mediated silencing in RI.** DAT-Cre lactating females expressing eNpHR3 or control
601 eYFP were introduced to between one to four juvenile female intruders, in 3 acclimation sessions
602 without photostimulation to assess baseline aggression as well as to augment aggressiveness.
603 Testing sessions initiated with recordings in the absence of laser stimulation to assess baseline
604 behavior towards each intruder on the day of the experiment. In photostimulation trials, irradiance
605 (intensity) ranging from 2.1 – 11.6 mW/mm^2 was delivered continuously in varying intervals (typically
606 2-10 sec) depending on the phase of the resident-intruder interaction. To examine whether
607 photostimulation during charging stopped escalation to attack, residents were photostimulated during
608 body realignment to gain access to the back of the intruder.
609
610 **Pup retrieval test.** Adult virgin female or lactating mice 5-8 months old were exposed to foster
611 pups or to their own litter, respectively. The litter size per test is described in the individual
612 tests/figures. Material for nest building was provided in each cage. The activity in the cage was video
613 recorded, and maternal behaviors were scored by an experimenter blinded to the experimental
614 conditions.
615
616 **Three-chambered sociability test.** The social approach apparatus was an open-topped box
617 made of acrylic (60 cm in length × 40 cm in width × 20 cm in height), and divided into three chambers
618 with two clear acrylic walls. Dividing walls had retractable doorways allowing access into each
619 chamber. The wire cup used to contain the novel mice was made of cylindrical chrome bars spaced
620 1 cm apart (10 cm H; bottom diameter: 10 cm). Test mice were confined in the center chamber at the
621 beginning of each phase. Exploration of an enclosed mouse or an empty wire cup was defined as
622 when a test mouse oriented toward the cup with the distance between the nose and the cup less than
623 1 cm, or as climbing on the cup. The time spent in each chamber and time spent exploring enclosed
624 novel mice or empty cups (the novel objects) were recorded from an overhead camera, and analyzed
625 using Ethovision XT12.
626

627 **Open field test (OFT).** OFTs were performed in a white acrylic glass box (45 × 45 × 40 cm) with
628 an overhead lamp directed to the centre of the field, providing 120 lux of illumination on the floor of
629 the arena. Each mouse was placed in the corner of the apparatus and locomotion parameters were
630 recorded for 20 min.
631
632 **Elevated plus maze (EPM).** The EPM test was performed using a polyvinyl chloride maze
633 comprising a central part (5x5 cm), two opposing open arms (32.5x5 cm), and two opposing closed
634 arms (32.5x5x32.5 cm). The apparatus was set to a height of 50 cm, and the open arms were provided
635 with uniform overhead illumination of 6 lux. Mice were placed in the open arm point close to the centre
636 facing the closed arms, and video recordings were performed for a total duration of 20 min.
637
638 **Chronic administration of maternal hormones in the PMv.** For localized chronic administration
639 of maternal hormones in the PMv, we performed cannula implantations using the Paxinos and
640 Franklin atlas (*102*) coordinates (Bregma: -2.45 mm, midline ±0.6 mm, dorsal surface -5.5 mm).
641 Cannulae (0008663 Brain Infusion Kit 2) and osmotic minipumps (0000298 ALZET Model 2004) were
642 purchased from ALZET, and prepared according to protocol.
643
644 **Brain slice electrophysiology.** Acute slices of the mediobasal hypothalamus were prepared
645 from adult DAT-tdTomato mice (own breeding). Slices were cut on a vibratome (Leica VT1000S) to
646 250 µm thickness and continuously perfused with oxygenated aCSF containing (in millimolar): NaCl
647 (127), KCl (2.0), NaH_2PO_4 (1.2), $NaHCO_3$ (26), $MgCl_2$ (1.3), $CaCl_2$ (2.4), and D-glucose (10), at room
648 temperature during recording. Each slice was exposed only to a single bath application of
649 pharmacological compounds and was used for a single experiment. Whole-cell current- and voltage-
650 clamp recordings were performed with micropipettes filled with intracellular solution containing (in
651 millimolar), K-gluconate (140), KCl (10), HEPES (10), EGTA (10), and Na_2ATP (2) (pH 7.3 with KOH).
652 Recordings were performed using a Multiclamp 700B amplifier, a DigiData 1440 digitizer, and pClamp
653 10.2 software (Molecular Devices, San Jose, CA, USA). Slow and fast capacitative components were
654 semi-automatically compensated. Access resistance was monitored throughout the experiments, and
655 neurons in which the series resistance exceeded 15 MΩ or changed ≥20% were excluded from the
656 statistics. Liquid junction potential was 16.4 mV and not compensated. The recorded current was
657 sampled at 20 kHz.
658 Reagents used in slice electrophysiology experiments; Neurobiotin™ tracer (Vector laboratories)
659 was used in combination with Streptavidin, DyLight™ 405 conjugated (21831 Thermoscientific) or
660 Avidin-FITC (43-4411 Invitrogen). TTX was purchased from Alomone Labs. Oxytocin nonapeptide,
661 the OT-receptor (OT-R) agonist, (Thr4, Gly7)-oxytocin (TGOT), and the oxytocin receptor antagonist,
662 vasotocin [d$(CH2)_5^1$, Tyr$(Me)^2$, Thr^4, Orn^8, des-Gly NH_2^9] (OR-A), were purchased from Bachem.
663 Prolactin CYT-321 was purchased from PROSPEC, and SR 95531 (Gabazine) and ML-218

664 hydrochloride were purchased from Tocris. Matlab and OriginPro8 were used for electrophysiological
665 data analysis.
666
667 **Immunofluorescence.** Mice were anaesthetised with sodium pentobarbital (200 mg/kg, i.p.,
668 Sanofi-Aventis, France), then transcardially perfused with 10 mL Ca^{2+}-free Tyrode's solution (37°C)
669 containing 0.2% heparin, followed by 10 mL fixative (4% paraformaldehyde and 0.4% picric acid in
670 0.16 M phosphate buffer (PBS), 37°C), then 50 mL ice cold fixative. Whole brains were dissected,
671 immersed in ice cold fixative for 90 min then stored in 0.1M PBS (pH 7.4) containing 20% sucrose,
672 0.02% bacitracin and 0.01% sodium azide for three days, before freezing with CO_2. Coronal sections
673 were cut at a thickness of 14 µm on a cryostat (Microm, Walldorf) and thaw-mounted onto gelatin-
674 coated glass slides. For indirect immunofluorescence staining (performed at room temperature unless
675 otherwise specified), air-dried sections were washed in 0.01 M PBS for 30 min before incubation with
676 primary antisera diluted in PBS containing 0.3% Triton X-100 and 1% BSA for 16 hours at 4°C. The
677 slides were then washed for 30 min in PBS followed by 2h incubation with Alexa-488-conjugated
678 donkey anti-rabbit secondary antisera (1:500; Invitrogen). Slides went through a final wash for 30 min
679 in PBS and mounted with glycerol containing (2.5% DABCO; Sigma, St Louis). This method was used
680 with the following antibodies: NeuN was detected with primary antibody rabbit anti-NeuN (1:500; Cell
681 Signalling, D4G40), eYFP was detected with chicken anti-GFP (1:500; Aves Labs, GFP-1020).
682 Immunohistochemistry for pSTAT5: Prior to immunofluorescence staining, antigen retrieval was
683 performed by incubating sections for 15 min in citric acid (pH 7.4) at 80°C, then cooled at room
684 temperature for a further 30 min. After a 1% H_2O_2 Tris-buffered wash, sections were incubated in
685 rabbit pSTAT5 primary antibody (pSTAT5 Tyr 694, Cat#: C11C5, 1:500; Cell Signaling Technology)
686 for 72 hours at 4°C. Primary antibody incubation was followed by Alexa-488-conjugated donkey anti-
687 rabbit secondary antisera (1:500; Invitrogen).
688 To perform c-fos immunostaining, mice were deeply anesthetized with sodium pentobarbital (as
689 described above) and perfused transcardially with 4% (weight/vol) ice-cold paraformaldehyde in 0.1M
690 PBS. Brains were post-fixed in the same solution and 40 µm-thick coronal slices were cut at the
691 vibratome (Leica, Germany). Two PMv coronal sections per animal were selected to perform c-fos
692 immunostaining as follows. Sections were washed in TBS (100 mM Tris-Cl, 150 mM NaCl, pH 7.5),
693 incubated 1h at 25ºC in 1% BSA-0.3% Triton X-100-TBS solution and then kept at 4°C in rabbit anti-
694 c-fos antibody (sc-52 LotG1108, Santa Cruz Biotechnology) solution (1:200 in 1% BSA-TBS)
695 overnight. After TBS washing, sections were incubated for 1h at 25ºC in Alexa Fluor® 647 (Invitrogen)
696 goat anti-rabbit secondary antibody (1:500 in 1% BSA-TBS).
697
698 **Microscopy and cell-counting.** All brain slices were imaged by epifluorescence microscopy
699 (ZEISS Imager M1) or confocal microscopy (Zeiss, LSM 800) for subsequent analysis. Brain areas
700 were determined according to their anatomy using Paxinos and Franklin Brain Atlas(*102*). For PMv^{DAT}

701 cell counts the entire PMv was cut, stained and counted. Quantification of c-fos staining was obtained
702 by averaging the number of positive cells of right and left PMv in two brain sections (-2.46 and -2.54
703 from Bregma)(*102*). All counts were performed manually using Image J software and blind to test
704 conditions.
705
706 **Randomization and blinding.** Behavioral data collection and analysis was performed blind to
707 experimental conditions. Anatomy data analysis but not tissue collection was blinded.
708 Electrophysiological data sampling and analysis was not blinded, with the exception of all whole-cell
709 patch clamp datasets presented in Figure 1. Mice were first screened for expressing maternal
710 aggression and then further assigned to groups for behavioral experiments.
711
712 **Statistical analysis.** No statistical methods were used to pre-determine sample sizes but our
713 sample sizes are similar to those reported in previous publications[2, 11, 14, 30, 31]. Data met the
714 assumptions of the statistical tests used, and were tested for normality and equal variance. All *t*-tests
715 and one-way ANOVAs were performed using Graph Pad Prism software (Graphpad Software Inc.).
716 The Tukey and Bonferroni *posthoc* tests were used as appropriate for one-way ANOVAs. Normality
717 was determined by D'Agostino–Pearson normality test. Statistical significance was set at $P < 0.05$.
718
719 **Data availability statement.** The data that support the findings of this study are available from
720 the corresponding authors upon request.

Figures

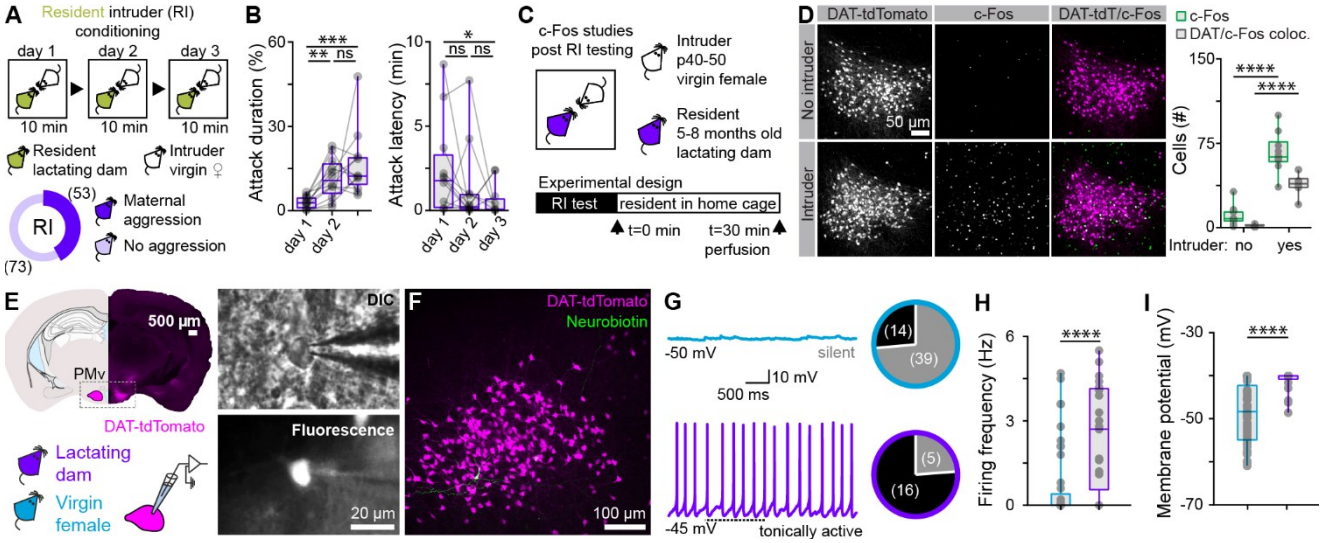

Figure 1. PMv^{DAT} neurons activate in lactating dams following an aggressive encounter and are electrically hyperexcitable during nursing state.

(A) Schematic representation of the experimental design used to identify lactating dams expressing maternal aggression (n = 126 lactating mice). Lactating dams were between five and eight months of age.

(B) Quantification of maternal aggression traits identify increased attack duration (left; shown as the percentage of total session time) and decreased attack latency (right) with consecutive trials in the RI paradigm shown in Figure 1A (n = 15 mice per group, RM one-way ANOVA, p = 0.0010).

(C) Schematic representation of the experimental design used to perform c-Fos studies following RI testing.

(D) Confocal images of c-Fos immunoreactivity in PMv, in the absence (top panels) or presence (bottom panels) of a juvenile female conspecific post-RI testing (n = 12 sections from 6 mice without intruder exposure, and n = 10 sections from 5 mice with intruder exposure; comparisons performed using two-tailed unpaired *t*-test, p < 0.0001).

(E) Identification of PMv^{DAT} neurons using the DAT-tdTomato mouse line to perform whole-cell patch clamp slice recordings from age-matched adult virgin female and lactating mice (five to eight months old).

(F) PMv^{DAT} neurons were identified and reconstructed post the recording session using Neurobiotin-FITC.

(G) Example recordings from PMv^{DAT} neurons (left) and group data in pie charts (right) from virgin female (blue) and lactating (purple) mice, exhibiting low (gray) *vs* high (black) baseline spike discharge, respectively (n = 53 and 21 recorded cells from 26 virgin female and 11 lactating dams, respectively).

(H) Quantification of firing frequency in PMv^{DAT} cells in virgin females *vs* lactating dams (n = 21-53 cells, two-tailed unpaired t-test, p < 0.0001).

756 (I) Quantification of membrane potential in PMv^{DAT} cells in virgin females *vs* lactating dams (n = 21-
757 53 cells, two-tailed unpaired t-test, $p < 0.0001$).
758 See also Table S1.

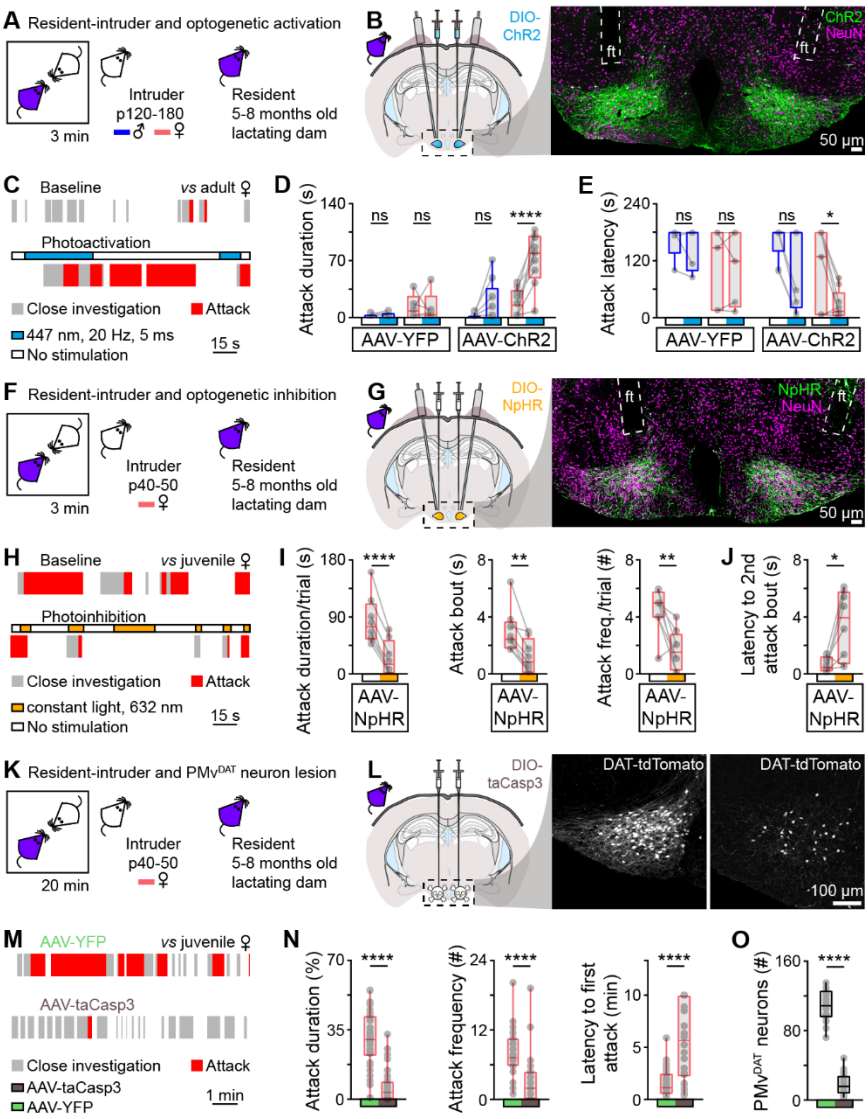

Figure 2. Manipulation of the PMv^{DAT} neuron activity allows bidirectional control of maternal aggression.

(A) Schematic of the experimental design used to perform ChR2 PMv^{DAT} neuron photoactivation in the resident lactating dam during resident-intruder (RI) testing. Adult male and female intruders were used to decrease the levels of maternal aggression expressed in baseline conditions (*38, 45*).

(B) Bilateral Cre-dependent ChR2 transfection and fiber implants in the PMv of lactating dams (left) and confocal image of a sample section counterstained with the pan-neuronal marker NeuN, used to validate ChR2 expression and stereotactic implantation coordinates (right).

(C) Sample behavior raster plots at baseline (top) and during ChR2 stimulation (bottom) in a lactating dam during a RI test.

(D) Attack duration with and without photostimulation in lactating dams injected with eYFP or ChR2, during the RI test against adult male or adult female intruders (n = 5-9 mice per group, ordinary one-way ANOVA, $p < 0.0001$).

790 (E) Attack latency with and without photostimulation in lactating dams injected with eYFP or ChR2,
791 during the RI test against adult male or adult female intruders (n = 5-9 mice per group, ordinary one-
792 way ANOVA, p = 0.0027).
793 (F) Schematic of the experimental design used to perform eNpHR3 PMv^{DAT} neuron photoinhibition
794 studies in the resident lactating dam during RI testing.
795 (G) Bilateral Cre-dependent eNpHR3 transfection and fiber implants in the PMv of lactating dams
796 (left) and confocal image of a sample section counterstained with the pan-neuronal marker NeuN,
797 used to validate eNpHR3 expression and stereotactic implantation coordinates (right).
798 (H) Sample behavior raster plots during baseline and eNpHR3 mediated photoinhibition in a lactating
799 dam during a RI test.
800 (I) Quantification of aggression parameters (n = 8 mice per group, two-tailed paired t-test).
801 (J) Quantification of the latency to an attack bout following a photoinhibition episode (n = 8 mice per
802 group, two-tailed paired t-test, p = 0.0131).
803 (K) Schematic of the experimental design used to perform RI tests in lactating dams with complete or
804 partial lesion of the PMv^{DAT} cells.
805 (L) Bilateral Cre-dependent taCasp3 transfection in the PMv of lactating dams (left) and sample
806 confocal image sections following injection of eYFP (middle) *vs* taCasp3 (right), used to validate the
807 extent of the PMv^{DAT} cell lession.
808 (M) Sample behavior raster plots in control *vs* PMv^{DAT} neuron lesioned lactating dams during a RI
809 test.
810 (N) Quantification of aggression parameters (n = 34 trials per group, 12 mice per group, two-tailed
811 unpaired t-test). All but 2 mice were tested three times in the RI test. Two mice, one from each group,
812 were tested two times in the RI test.
813 (O) Quantification of PMv^{DAT} neurons in eYFP and taCasp3 injected mice (n = 24 sections per group,
814 duplicates from 12 mice per group, two-tailed unpaired t-test, p < 0.0001).
815 See also Table S1, and Figure S1.

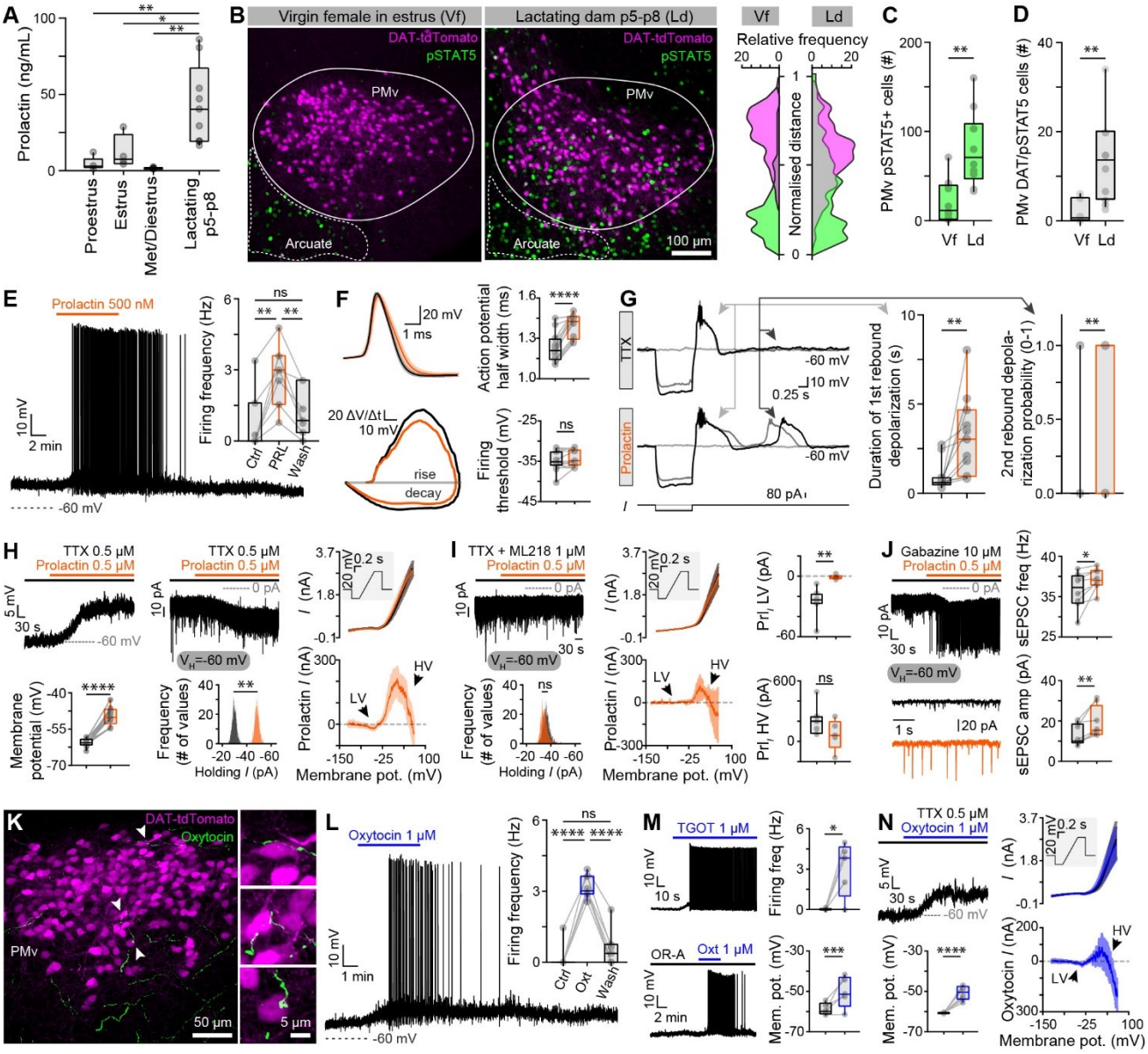

Figure 3. Maternal hormones activate PMv^{DAT} neurons.

(A) Serum prolactin levels in virgin females across the estrous cycle (proestrus, estrus, met-/diestrus) *vs* lactating dams (n = 4-9 mice per group, ordinary one-way ANOVA, p = 0.0007).

(B) Confocal images of pSTAT5 immunoreactivity in PMv, in virgin females in estrus *vs* lactating dams (left). Overlap of pSTAT5 and DAT-tdTomato fluorescence along the Y axis, with 0 being the most ventral point of the confocal image and 1 the most dorsal (right).

(C) Quantification of pSTAT5 immunoreactive cells in the PMv of virgin females in estrus *vs* lactating dams (n = 10 sections per group, 5 mice per group, 2 sections per mouse, two-tailed unpaired t-test, p = 0.0011).

(D) Quantification of DAT-tdTomato colocalizing pSTAT5 immunoreactive cells in the PMv of virgin females in estrus *vs* lactating dams (n = 10 sections per group, 5 mice per group, 2 sections per mouse, two-tailed unpaired t-test, p = 0.0015).

829 (E) Prolactin leads to a reversible depolarization of PMv^{DAT} neurons (n = 7 cells from 5 mice, RM one-
830 way ANOVA, p = 0.0016).
831 (F) Prolactin induced changes in the action potential waveform of PMv^{DAT} neurons (left). Quantification
832 of action potential (AP) half-width and firing threshold in control (black) *vs* prolactin (orange, n = 15
833 action potentials in control *vs* bath application of prolactin per cell, 7 cells from 5 mice, two-tailed
834 paired t-test).
835 (G) (left) Comparison of post-inhibitory rebound bouts in control (TTX) *vs* prolactin application (TTX +
836 prolactin). Black traces represent the hyperpolarization induced by the highest absolute amplitude
837 negative current pulse, with the effect of a smaller amplitude pulse illustrated in dark gray and the
838 absence of any pulse in light gray. (middle) Quantification of the 1st post-inhibitory rebound in control
839 (black) *vs* prolactin (orange, n = 11 cells per group collected from 6 mice, two-tailed paired t-test, p =
840 0.0098). (right) Quantification of a 2nd post-inhibitory rebound probability in control (black) *vs* prolactin
841 (orange, n = 11 cells per group collected from 6 mice, two-tailed paired t-test, p = 0.0061).
842 (H) Identification of a prolactin induced postsynaptic depolarization on PMv^{DAT} cells in current clamp
843 (left, n=13 cells per group collected from 8 mice, two-tailed paired t-test, p < 0.0001) and voltage
844 clamp (middle, n = 5 cells per group collected from 5 mice, two-tailed paired t-test, p = 0.0078).
845 Characterization of the prolactin induced current across the membrane voltage spectrum in PMv^{DAT}
846 neurons, with a low- and high-voltage component (right, n = 7 cells collected from 4 mice).
847 (I) Application of the selective T-type Ca^{2+} current blocker ML218, blocks the low-voltage component
848 of the prolactin induced current (Prl_I). Application of prolactin does not induce an inward current in
849 PMv^{DAT} neurons pre-exposed to ML218 (left, n = 6 cells per group collected from 4 mice, two-tailed
850 paired t-test, p = 0.5129). In the presence of ML218 the prolactin induced current is composed only
851 of a high-voltage component (middle, n = 6 cells collected from 4 mice). Comparison of the low- (right,
852 n=6-7 cells per group, two-tailed unpaired t-test, p = 0.0042) and high-voltage (right, n=6-7 cells per
853 group, two-tailed unpaired t-test, p = 0.1384) component of the prolactin induced current in the
854 absence *vs* presence of ML218.
855 (J) Electrophysiology recordings of spontaneous excitatory postsynaptic currents during gabazine (for
856 blocking spontaneous inhibitory postsynaptics currents) and application of Prl (n = 8 cells collected
857 from 4 mice).
858 (K) Oxytocin-immunoreactive fibers forming close appositions to PMv^{DAT} neurons (n = 5 mice).
859 (L) Oxytocin leads to a reversible depolarization of PMv^{DAT} neurons (n = 7 cells per group, collected
860 from 5 mice, RM one-way ANOVA, p < 0.0001).
861 (M) Application of the selective oxytocin receptor agonist, TGOT, leads to depolarization of PMv^{DAT}
862 neurons (top, n = 5 cells per group, collected from 5 mice, two-tailed paired t-test, p = 0.0274).
863 Application of oxytocin under oxytocin receptor blockade, leads to depolarization of PMv^{DAT} neurons
864 (bottom, n = 5 cells per group, collected from 5 mice, two-tailed paired t-test, p = 0.0008).

865 (N) Identification of an oxytocin induced postsynaptic depolarization on PMv^{DAT} cells in current clamp
866 (left, n=8 cells per group collected from 4 mice, two-tailed paired t-test, $p < 0.0001$). Characterization
867 of the oxytocin induced current across the membrane voltage spectrum in PMv^{DAT} neurons, with a
868 low- and high-voltage component (right, n = 8 cells collected from 4 mice).
869 See also Table S1.

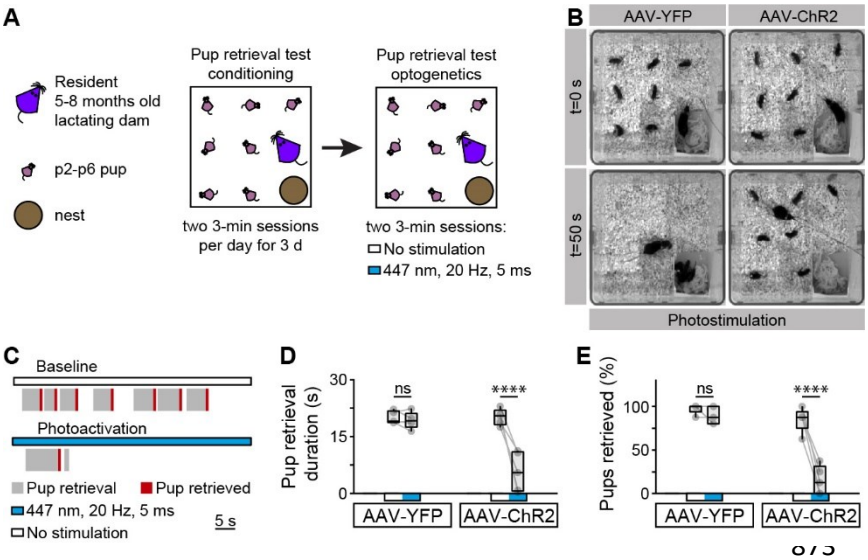

Figure 4. Activation of PMv^{DAT} neurons suppresses non-aggression-related behavioral programs.

(A) Schematic of the experimental design used to perform ChR2 PMv^{DAT} neuron photoactivation during the pup retrieval test.

(B) Images from two photostimulation trials at the start (0 s) and 50 s *post*-trial initiation, with lactating dams expressing eYFP (left) and ChR2 (right) in PMv^{DAT} neurons.

(C) Sample behavior raster plots of two sequential trials without and with photostimulation in a ChR2-expressing lactating dam during the pup retrieval test.

(D) Pup retrieval duration with and without photostimulation in lactating dams injected with eYFP or ChR2, during the pup retrieval test (n = 5 mice per group, ordinary one-way ANOVA, $p < 0.0001$).

(E) Percentage of pups retrieved with and without photostimulation in lactating dams injected with eYFP or ChR2, during the pup retrieval test (n = 5 mice per group, ordinary one-way ANOVA, $p < 0.0001$).

See also Table S1.

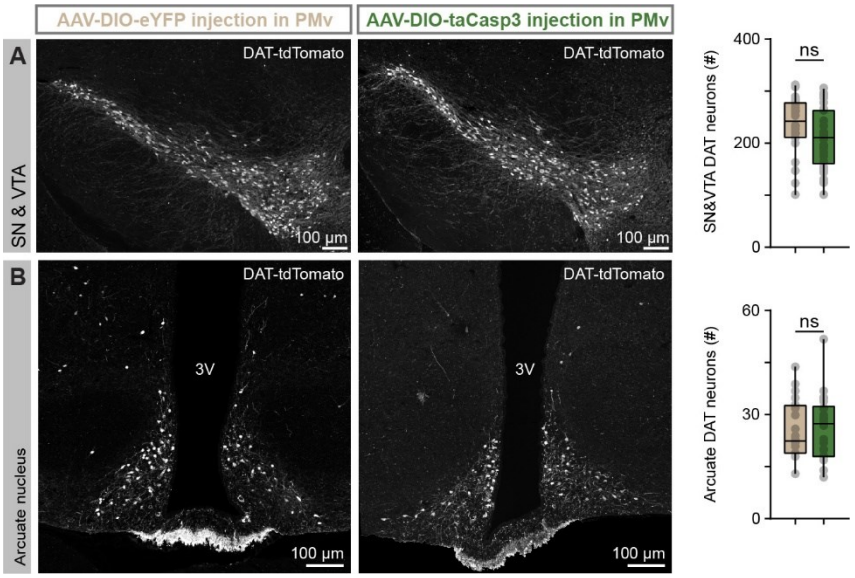

Figure S1. Injection of AAV-flex-taCasp3 in the PMv of DAT-Cre animals does not extend across the rostrocaudal axis, leaving the midbrain and arcuate nucleus dopamine neurons unaffected, related to Figure 2.

(A) Confocal image of an eYFP- (left) *vs* taCasp3- (middle) PMv injected sample sections of midbrain (substantia nigra, SN, and ventral tegmental area, VTA) DAT-tdTomato neurons, and quantification of cell number per section (n = 24-26 sections per group, duplicates from 12-13 mice per group, two-tailed unpaired t-test, p = 0.1141).

(B) Confocal image of an eYFP- (left) *vs* taCasp3- (middle) PMv injected sample sections of arcuate DAT-tdTomato neurons, and quantification of cell number per section (n = 24-26 sections per group, duplicates from 12-13 mice per group, two-tailed unpaired t-test, p = 0.5650). 3V, third ventricle. See also Table S1.

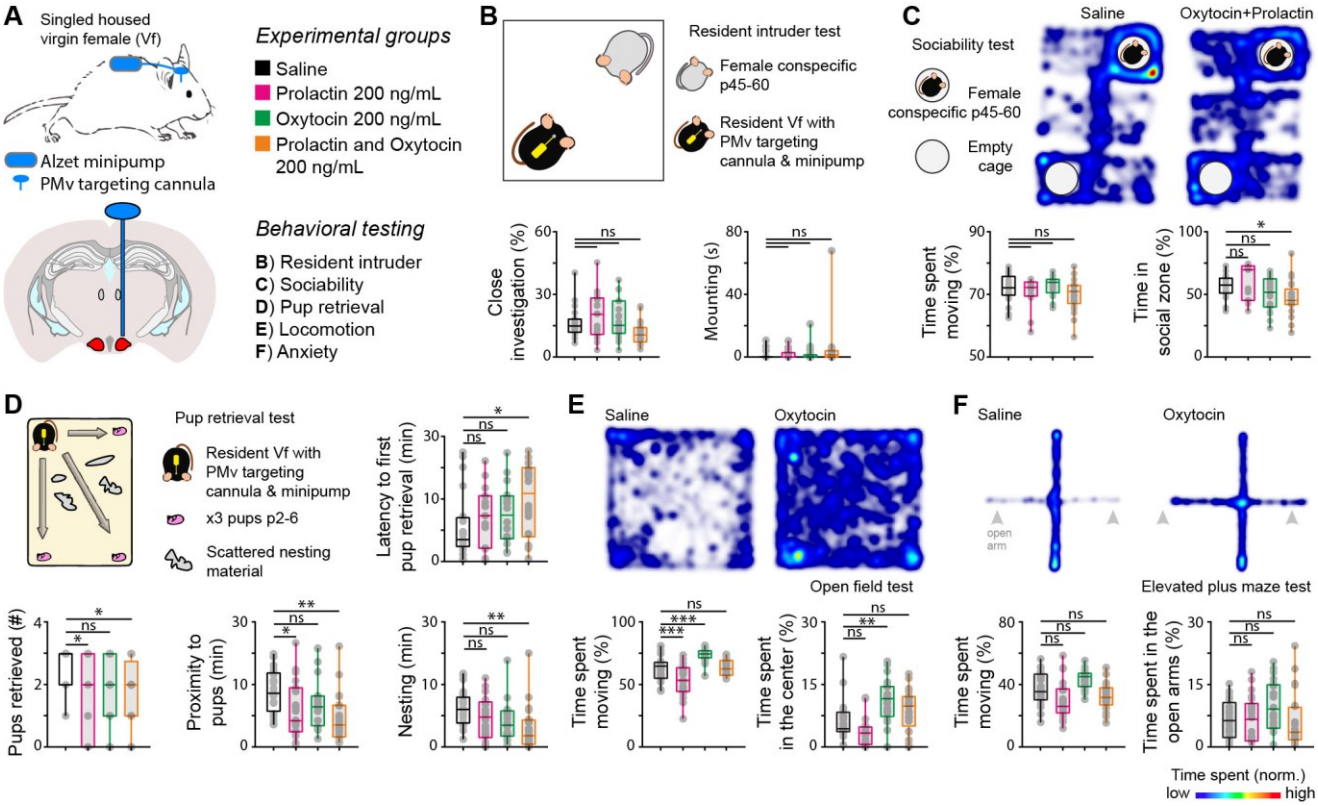

Figure S2. Chronic administration of maternal hormones in PMv is not sufficient to evoke aggression in virgin females, related to Figure 3.

(A) Schematic of the experimental design followed to infuse maternal hormones into the PMv parenchyma via cannulas for a period of 28 days, and perform a panel of behavioral tests.

(B) Quantification of social behaviors in the RI test, with implanted resident adult virgin females *vs* juvenile virgin female intruders. No changes in close investigation or mounting duration were recorded (n = 21-24 trials per group, triplicates from 7-8 mice per group, RM one-way ANOVA). No episodes of aggression occurred in any of the groups.

(C) Design and results from the sociability test, where implanted adult virgin female mice can choose between an empty chamber and one with a juvenile virgin female conspecific present. (n = 13-24 trials per group, duplicates or triplicates from 7-8 mice per group, ordinary one-way ANOVA).

(D) Design and results from the pup retrieval test, with implanted adult virgin female mice (n = 21-24 trials per group, triplicates from 7-8 mice per group, ordinary one-way ANOVA).

(E) Results from the open field test, with implanted adult virgin female mice (n = 21-24 trials per group, triplicates from 7-8 mice per group, ordinary one-way ANOVA).

(F) Results from the elevated plus maze test, with implanted adult virgin female mice (n = 21-24 trials per group, triplicates from 7-8 mice per group, ordinary one-way ANOVA). See also Table S1.

924 Table S1

Figures	Test	n (per group)	KW statistic or t values	df	p value	Comparisons	Adjusted p value	p value summary
Figure 1B, left – attack duration (%)	RM one-way ANOVA with Kruskal-Wallis post-hoc test	12	KW statistic = 18.18	11	0.0001	day 1 *vs*. day 2	0.0051	**
						day 1 *vs*. day 3	0.0001	***
						day 2 *vs*. day 3	>0.9999	ns
Figure 1B, right – attack latency (s)	RM one-way ANOVA with Kruskal-Wallis post-hoc test	12	KW statistic = 7.182	11	0.0276	day 1 *vs*. day 2	0.2988	ns
						day 1 *vs*. day 3	0.0238	*
						day 2 *vs*. day 3	0.9411	ns
Figure 1D, c-Fos cells (#)	Two-tailed unpaired t-test	10-12	t = 9.661	20	< 0.0001	c-Fos in PMv without *vs.* with intruder	N/A	****
Figure 1D, DAT/c-Fos cells (#)			t = 11.72			DAT/c-Fos colocalization without *vs.* with intruder	N/A	****
Figure 1H, firing frequency (Hz)	Two-tailed unpaired t-test	21-53	t = 4.540	72	< 0.0001	virgin *vs.* lactating	N/A	****

925

926

Figures	Test	n (per group)	F or t values	df	p value	Comparisons	Adjusted p value	p value summary
Figure 2D, attack duration (s)	Ordinary one-way ANOVA with uncorrected Fisher's LSD test as multiple comparisons test	5-9	$F_{(7, 48)} = 11.55$	7	< 0.0001	AAV-eYFP dam, against adult virgin male intruder – baseline *vs.* photostimulation	> 0.9999	ns
						AAV-eYFP dam, against adult virgin female intruder – baseline *vs.* photostimulation	> 0.9999	ns
						AAV-ChR2 dam, against adult virgin male intruder – baseline *vs.* photostimulation	> 0.9999	ns
						AAV-ChR2 dam, against adult virgin female intruder – baseline *vs.* photostimulation	< 0.0001	****
Figure 2E, attack latency (s)	Ordinary one-way ANOVA with uncorrected Fisher's LSD test as multiple comparisons test	5-9	$F_{(7, 48)} = 3.732$	7	0.0027	AAV-eYFP dam, against adult virgin male intruder – baseline *vs.* photostimulation	0.7149	ns
						AAV-eYFP dam, against adult virgin female intruder – baseline *vs.* photostimulation	0.9468	ns
						AAV-ChR2 dam, against adult virgin male intruder – baseline *vs.* photostimulation	0.1043	ns
						AAV-ChR2 dam, against adult virgin female intruder – baseline *vs.* photostimulation	0.0266	*

927

Figures	Test	n (per group)	F or t values	df	p value	Comparisons	Adjusted p value	p value summary
Figure 2I, left attack duration/trial (s)	Two-tailed paired t-test	8	t = 9.280	7	< 0.0001	AAV-ChR2 dam, against a juvenile virgin female intruder – baseline *vs.* photostimulation	N/A	****
Figure 2I, middle attack bout (s)	Two-tailed paired t-test	8	t = 5.356	7	0.0011	AAV-ChR2 dam, against a juvenile virgin female intruder – baseline *vs.* photostimulation	N/A	**
Figure 2I, right attack frequency/trial (#)	Two-tailed paired t-test	8	t = 3.752	7	0.0071	AAV-ChR2 dam, against a juvenile virgin female intruder – baseline *vs.* photostimulation	N/A	**
Figure 2J, latency to first attack following a photoinhibition episode (s)	Two-tailed paired t-test	8	t = 3.300	7	0.0131	AAV-ChR2 dam, against a juvenile virgin female intruder – baseline *vs.* photostimulation	N/A	*
Figure 2N, left attack duration (%)	Two-tailed unpaired t-test	34	t = 8.827	54	< 0.0001	against a juvenile virgin female intruder – eYFP *vs.* taCasp3 injected lactating dams	N/A	****
Figure 2N, middle attack frequency (#)	Two-tailed unpaired t-test	34	t = 5.348	66	< 0.0001	against a juvenile virgin female intruder – eYFP *vs.* taCasp3 injected lactating dams	N/A	****
Figure 2N, right latency to first attack (min)	Two-tailed unpaired t-test	34	t = 6.506	41	< 0.0001	against a juvenile virgin female intruder – eYFP *vs.* taCasp3 injected lactating dams	N/A	****
Figure 2O, PMv^{DAT} neurons (#)	Two-tailed unpaired t-test	24	t = 22.78	48	< 0.0001	eYFP *vs.* taCasp3 injected lactating dams	N/A	****

928

Figures	Test	n (per group)	F or t values	df	p value	Comparisons	Adjusted p value	p value summary
Figure 3A, Serum Prolactin (ng/mL)	Ordinary one-way ANOVA with Dunnett's multiple comparisons test	4-9	$F_{(3, 19)} = 8.797$	3	0.0007	proestrus *vs.* lactating	0.0022	**
						estrus *vs.* lactating	0.0199	*
						met-/diestrus *vs.* lactating	0.0011	**
Figure 3C, pSTAT5 cells in PMv (#)	Two-tailed unpaired t-test	10	t = 3.878	18	0.0011	Virgin in estrus *vs.* lactating	N/A	**
Figure 3D, PMv^{DAT}/pSTAT5 cell colocalization (#)	Two-tailed unpaired t-test	10	t = 3.737	18	0.0015	Virgin in estrus *vs.* lactating	N/A	**
Figure 3E, firing frequency (Hz)	RM one-way ANOVA with Bonferroni's multiple comparisons test	7	$F_{(1.723, 10.34)} = 13.73$	6	0.0016	control *vs.* prolactin	0.0069	**
						control *vs.* wash	> 0.9999	ns
						prolactin *vs.* wash	0.0097	**
Figure 3F, action potential half width (ms)	Two-tailed paired t-test	15	t = 8.847	14	< 0.0001	control *vs.* prolactin	N/A	****
Figure 3F, action potential firing threshold (mV)	Two-tailed paired t-test	15	t = 1.926	14	0.0746	control *vs.* prolactin	N/A	ns
Figure 3G, duration of 1st rebound depolarization (s)	Two-tailed paired t-test	11	t = 3.183	10	0.0098	control *vs.* prolactin	N/A	**
Figure 3G, 2nd rebound depolarization probability	Two-tailed paired t-test	11	t = 3.464	10	0.0061	control *vs.* prolactin	N/A	**
Figure 3H, left membrane potential (mV)	Two-tailed paired t-test	13	t = 9.753	12	< 0.0001	control *vs.* prolactin	N/A	****
Figure 3H, middle Holding I (pA)	Two-tailed paired t-test	5	t = 4.941	4	0.0078	control *vs.* prolactin	N/A	**
Figure 3I, left Holding I (pA)	Two-tailed paired t-test	6	t = 0.7040	5	0.5129	control *vs.* prolactin	N/A	ns

Figure 3I, top right Prl/ LV(pA)	Two-tailed unpaired t-test	5-7	t = 3.685	10	0.0042	control *vs.* prolactin	N/A	**
Figure 3I, bottom right Prl/ LV(pA)	Two-tailed unpaired t-test	5-7	t = 1.611	10	0.1384	control *vs.* prolactin	N/A	ns
Figure 3J, top right sEPSC frequency (Hz)	Two-tailed paired t-test	8	t = 3.609	7	0.014	control *vs.* prolactin	N/A	*
Figure 3J, bottom right sEPSC amplitude (pA)	Two-tailed paired t-test	8	t = 4.069	7	0.0048	control *vs.* prolactin	N/A	**
Figure 3L, firing frequency (Hz)	RM one-way ANOVA with Bonferroni's multiple comparisons test	7	$F_{(1.114, 6.682)} = 75.40$	6	< 0.0001	control *vs.* oxytocin	< 0.0001	****
						control *vs.* wash	> 0.9999	ns
						oxytocin *vs.* wash	< 0.0001	****
Figure 3M, top firing frequency (Hz)	Two-tailed paired t-test	5	t = 3.393	4	0.0274	control *vs.* TGOT	N/A	*
Figure 3M, bottom membrane pot. (mV)	Two-tailed paired t-test	5	t = 9.253	4	0.0008	control *vs.* TGOT	N/A	***
Figure 3N, left membrane pot. (mV)	Two-tailed paired t-test	8	t = 8.040	7	< 0.0001	control *vs.* TGOT	N/A	****

929

Figures	Test	n (per group)	F or t values	df	p value	Comparisons	Adjusted p value	p value summary
Figure 4D, pup retrieval duration (s)	Ordinary one-way ANOVA with Bonferroni's multiple comparisons test	5	$F_{(3, 16)} = 25.59$	3	< 0.0001	AAV-eYFP dam – baseline *vs.* photostimulation	> 0.9999	ns
						AAV-ChR2 dam – baseline *vs.* photostimulation	< 0.0001	****
Figure 4E, pup retrieved (%)	Ordinary one-way ANOVA with Bonferroni's multiple comparisons test	5	$F_{(3, 16)} = 49.80$	3	< 0.0001	AAV-eYFP dam – baseline *vs.* photostimulation	> 0.9999	ns
						AAV-ChR2 dam – baseline *vs.* photostimulation	< 0.0001	****
Figure S1A, SN&VTA DAT neurons (#)	Two-tailed unpaired t-test	24-26	t = 1.609	48	0.1141	eYFP *vs.* taCasp3 injected lactating dams	N/A	ns
Figure S1B, arcuate DAT neurons (#)	Two-tailed unpaired t-test	24-26	t = 0.5794	48	0.5650	eYFP *vs.* taCasp3 injected lactating dams	N/A	ns
Figure S2B, close investigation (%)	RM one-way ANOVA with Bonferroni's multiple comparisons test	21-24	$F_{(3, 83)} = 3.760$	3	0.0138	saline *vs.* prolactin (Prl)	0.8239	ns
						saline *vs.* oxytocin (OT)	> 0.9999	ns
						saline *vs.* Prl & OT	0.1259	ns
Figure S2B, mounting (s)	RM one-way ANOVA with Bonferroni's multiple comparisons test	21-24	$F_{(3, 83)} = 0.9736$	3	0.4092	saline *vs.* prolactin (Prl)	> 0.9999	ns
						saline *vs.* oxytocin (OT)	> 0.9999	ns
						saline *vs.* Prl & OT	0.3291	ns
Figure S2C, time spent moving (%)	RM one-way ANOVA with Bonferroni's multiple comparisons test	13-24	$F_{(3, 75)} = 1.698$	3	0.1747	saline *vs.* prolactin (Prl)	> 0.9999	ns
						saline *vs.* oxytocin (OT)	> 0.9999	ns
						saline *vs.* Prl & OT	0.4069	ns
Figure S2C, time in social zone (%)	RM one-way ANOVA with Bonferroni's multiple comparisons test	13-24	$F_{(3, 75)} = 3.953$	3	0.0114	saline *vs.* prolactin (Prl)	> 0.9999	ns
						saline *vs.* oxytocin (OT)	0.2401	ns
						saline *vs.* Prl & OT	0.0346	*

Figures	Test	n (per group)	F or t values	df	p value	Comparisons	Adjusted p value	p value summary
Figure S2D, latency to first pup retrieval (min)	RM one-way ANOVA with Bonferroni's multiple comparisons test	15-20	$F_{(3, 65)} = 2.150$	3	0.1025	saline *vs.* prolactin (Prl)	> 0.9999	ns
						saline *vs.* oxytocin (OT)	0.8639	ns
						saline *vs.* Prl & OT	0.0418	*
Figure S2D, pups retrieved (#)	RM one-way ANOVA with Bonferroni's multiple comparisons test	20-24	$F_{(3, 82)} = 3.452$	3	0.0202	saline *vs.* prolactin (Prl)	0.0124	*
						saline *vs.* oxytocin (OT)	0.8639	ns
						saline *vs.* Prl & OT	0.0432	*
Figure S2D, proximity to pups (min)	RM one-way ANOVA with Bonferroni's multiple comparisons test	20-24	$F_{(3, 82)} = 4.716$	3	0.0044	saline *vs.* prolactin (Prl)	0.0330	*
						saline *vs.* oxytocin (OT)	0.3891	ns
						saline *vs.* Prl & OT	0.0017	**
Figure S2D, nesting (min)	RM one-way ANOVA with Bonferroni's multiple comparisons test	20-24	$F_{(3, 82)} = 3.819$	3	0.0129	saline *vs.* prolactin (Prl)	0.2276	ns
						saline *vs.* oxytocin (OT)	0.0669	ns
						saline *vs.* Prl & OT	0.0051	**
Figure S2E, time spent moving (%)	RM one-way ANOVA with Bonferroni's multiple comparisons test	21-24	$F_{(3, 83)} = 18.17$	3	< 0.0001	saline *vs.* prolactin (Prl)	0.0007	***
						saline *vs.* oxytocin (OT)	0.0009	***
						saline *vs.* Prl & OT	> 0.9999	ns
Figure S2E, time spent in the center (%)	RM one-way ANOVA with Bonferroni's multiple comparisons test	21-24	$F_{(3, 83)} = 10.59$	3	< 0.0001	saline *vs* prolactin (Prl)	0.1397	ns
						saline *vs.* oxytocin (OT)	0.0025	**
						saline *vs.* Prl & OT	0.1915	ns
Figure S2F, time spent moving (%)	RM one-way ANOVA with Bonferroni's multiple comparisons test	21-24	$F_{(3, 83)} = 7.991$	3	< 0.0001	saline *vs.* prolactin (Prl)	0.0697	ns
						saline *vs.* oxytocin (OT)	0.0578	ns
						saline *vs.* Prl & OT	0.4917	ns

Figures	Test	n (per group)	F or t values	df	p value	Comparisons	Adjusted p value	p value summary
Figure S2F, time spent in the open arms (%)	RM one-way ANOVA with Bonferroni's multiple comparisons test	21-24	$F_{(3, 83)} = 2.163$	3	0.0985	saline *vs.* prolactin (Prl)	> 0.9999	ns
						saline *vs.* oxytocin (OT)	0.1189	ns
						saline *vs.* Prl & OT	> 0.9999	ns

931